SPINE Volume 26, Number 14, pp 1547–1554
©2001, Lippincott Williams & Wilkins, Inc.

Effects of Bone Cement Volume and Distribution on Vertebral Stiffness After Vertebroplasty

Michael A.K. Liebschner, PhD,* William S. Rosenberg, MD,† and Tony M. Keaveny, PhD*‡

Study Design. The biomechanical behavior of a single lumbar vertebral body after various surgical treatments with acrylic vertebroplasty was parametrically studied using finite-element analysis.

Objectives. To provide a theoretical framework for understanding and optimizing the biomechanics of vertebroplasty. Specifically, to investigate the effects of volume and distribution of bone cement on stiffness recovery of the vertebral body.

Summary of Background Data. Vertebroplasty is a treatment that stabilizes a fractured vertebra by addition of bone cement. However, there is currently no information available on the optimal volume and distribution of the filler material in terms of stiffness recovery of the damaged vertebral body.

Methods. An experimentally calibrated, anatomically accurate finite-element model of an elderly L1 vertebral body was developed. Damage was simulated in each element based on empirical measurements in response to a uniform compressive load. After virtual vertebroplasty (bone cement filling range of 1–7 cm^3) on the damaged model, the resulting compressive stiffness of the vertebral body was computed for various spatial distributions of the filling material and different loading conditions.

Results. Vertebral stiffness recovery after vertebroplasty was strongly influenced by the volume fraction of the implanted cement. Only a small amount of bone cement (14% fill or 3.5 cm^3) was necessary to restore stiffness of the damaged vertebral body to the predamaged value. Use of a 30% fill increased stiffness by more than 50% compared with the predamaged value. Whereas the unipedicular distributions exhibited a comparative stiffness to the bipedicular or posterolateral cases, it showed a medial–lateral bending motion ("toggle") toward the untreated side when a uniform compressive pressure load was applied.

Conclusion. Only a small amount of bone cement (~15% volume fraction) is needed to restore stiffness to predamage levels, and greater filling can result in substantial increase in stiffness well beyond the intact level. Such overfilling also renders the system more sensitive to the placement of the cement because asymmetric distributions with large fills can promote single-sided load transfer and thus toggle. These results suggest that large fill volumes may not be the most biomechanically optimal configuration, and an improvement might be achieved by use of lower cement volume with symmetric placement.
[Key words: biomechanics, vertebroplasty, finite element, stiffness, bone damage] **Spine 2001;26:1547–1554**

From the *Orthopaedic Biomechanics Laboratory, Department of Mechanical Engineering, and the Departments of †Neurological Surgery, and ‡Bioengineering, University of California, Berkeley, California.
Supported by NSF BES-9625030, NIH AR41481, the University of California Academic Senate, and an unrestricted gift from Kyphon Inc., Santa Clara, California.
Acknowledgment date: September 12, 2000.
Acceptance date: December 14, 2000.
Device status category: 1.
Conflict of interest category: 15.

Augmentation of pathologic vertebral bodies with a bone filler material, typically polymethylmethacrylate (PMMA), constitutes a vertebroplasty.[3,13] Reported clinical studies have shown that even "insufficient" filling of vertebral bodies (<30% by volume of the vertebral body) during the vertebroplasty can lead to a successful outcome in pain reduction, stiffening and stabilizing of the fractured vertebrae.[8,10,16] In general, a large volume fraction of bone cement results in a stable (stiff) vertebral body due to the relatively high stiffness of bone cement compared with the vertebral trabecular bone. However, leakage of the cement outside the vertebral body has been reported to occur in more than 70% of cases, most frequently into the paraspinal soft tissue.[7–10,25] Although complication rates are relatively low (<6%),[23,35] most problems arise from leakage of the cement into the epidural, interbody, foraminal, or venous spaces, causing pulmonary embolus[25,28] or nerve root compression.[10] Thus, one important biomechanical issue for vertebroplasty is to minimize the amount of bone cement used and yet improve stiffness of the damaged vertebral body in a biomechanically significant manner; another issue is whether or not the spatial distribution of the introduced cement is an important consideration.

Little information is available on the biomechanical efficacy of unipedicular *versus* bipedicular vertebroplasty. Tohmeh et al[31] performed a cadaveric study on the biomechanics of osteoporotic fractured vertebral bodies treated with unipedicular vertebroplasty (6 cm^3 of bone cement) or bipedicular vertebroplasty (5 cm^3 of bone cement through each pedicle). Their results demonstrated that unipedicular and bipedicular vertebroplasty increased strength and restored stiffness of vertebral bodies with compression fractures. The experimental approach taken by Tohmeh et al,[31] however, did not address the effects of distribution or volume fraction of the filling material. Furthermore, the experimental limitations, including the constraint on specimen motion, did not allow for thorough investigation of the deformation behavior on the noninjected side for the unipedicular vertebroplasty cases. Compliance experiments on vertebroplasty treated spinal motion segments in lateral bending and flexion–extension have been performed and reported in the literature[36]; however, unipedicular approaches were not investigated, nor were the effects of changes of bone filler volume on bending compliance investigated. Indeed, there is currently no information available on the optimal protocols for such procedures, including the biomechanically optimal volume and placement of the filler material. Such information may

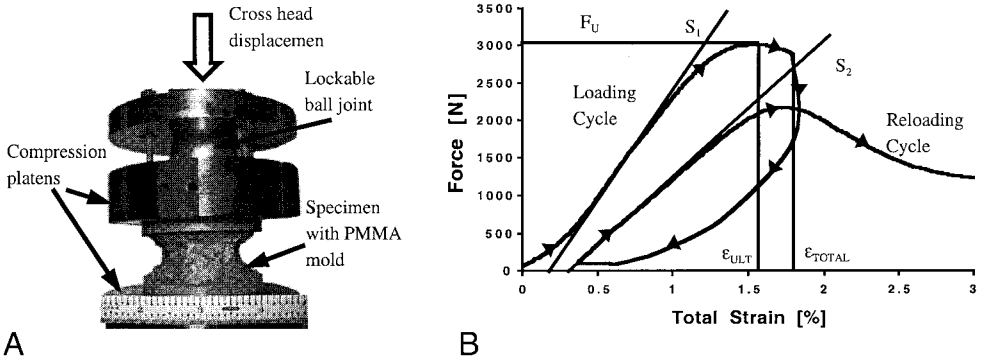

Figure 1. Load–reload experimental protocol and setup for vertebral body subject to uniaxial compression in servohydraulic testing machine. **A,** Compression platens with lockable ball joint allowed the top platen to rest flat on the specimen. **B,** Representative load–deformation curve of the loading, unloading, and reloading paths.

lead to refinement of the surgery, improved patient selection, and ultimately more confidence and successful use of this procedure.

The overall goal of this study was to provide a theoretical framework for understanding and optimizing the biomechanics of the vertebroplasty procedure. We developed an experimentally calibrated, anatomically detailed finite-element model from computed tomography scans, and simulations were made of various surgical approaches to vertebroplasty. Our specific objectives were as follows: 1) simulate the mechanical damage process in a human vertebral body for a static compressive load, 2) determine the sensitivity of compressive stiffness recovery of the damaged vertebral body to the volume and distribution of bone cement delivered, and 3) investigate the sensitivity of these trends to variations in the applied loading boundary conditions (stress *vs.* displacement constraints) for compressive loading.

■ Methods

A threefold approach was taken to develop a geometrically and biomechanically accurate model of a damaged and ultimately vertebroplasty treated human vertebral body. In the first part mechanical data were collected and evaluated from a single human vertebral body in a uniaxial compression experiment. The second part included generation of a finite-element model and validation of the model with respect to the experiment. The third part represented virtual simulations of four vertebroplasty treatment options used clinically with variations of bone cement volume and distribution. All analyses were performed on an L1 vertebral body of a 73-year-old cadaveric female, which was confirmed to be radiographically normal.

Biomechanical Testing. Before testing, the posterior elements and the intervertebral disc material were removed. Computed tomography (CT) scans of the vertebral body were taken on a GE 9800 scanner (General Electric, Milwaukee, WI). A liquid K_2HPO_4 calibration phantom (Mindways Software, Inc., San Francisco, CA) was included in each scan to correct for scanner drift and to convert CT numbers in Hounsfield units (HU) to bone mineral density (BMD) in g/cm^3. The vertebral body was kept hydrated with marrow *in situ* at all times and stored at −20 C between specimen preparation and mechanical testing.

In preparation for mechanical testing (see Kopperdahl et al[21] for details), PMMA was molded to the concave endplates of the vertebral body using a fixture that ensured plano-parallel ends. A compression test was performed between steel platens on a screw-driven load frame (Instron Corporation, Model 5583, Canton, MA) at room temperature (Figure 1A). After preconditioning, the specimen was loaded in displacement control at a rate of 0.15 mm/sec (~0.5% strain/sec) to an endpoint of 1.78% strain, equivalent to 0.593 mm cross-head displacement. This loading exceeded the ultimate point of the vertebral body. Strains were based on the initial height of the specimen, including PMMA, measured using a caliper, and recorded using a 2-inch extensometer (632.11F-20, MTS, Eden Prairie, MN) spanning the platens. The specimen was unloaded, held at a low compressive force (100 N) for 1 minute, and then reloaded to 10% strain.

Structural stiffness S was measured for both load cycles (Figure 1B) and was defined as the steepest slope of the load–deflection curve over a displacement range equivalent to 0.2% strain[21]; strength was defined as the maximum force (F_U) over the whole deflection range. Percent reduction in structural stiffness (%ΔS) was calculated relative to the initial cycle as follows[21]:

$$\%\Delta S = \frac{S_1 - S_2}{S_1} \times 100 \qquad (1)$$

where S_2 is the residual stiffness, measured on the reloading cycle and S_1 the intact stiffness.

Finite-Element Modeling. A finite-element model of the vertebral body was generated from the digitized CT scans using the TrueGrid software suite (XYZ Scientific Applications Inc., Livermore, CA), and stress analyses were performed using ABAQUS (Hibbit, Karlsson and Sorenson, Inc., Pawtucket, RI). The trabecular centrum was paved with 20-noded brick elements and assigned elastic moduli in the superior–inferior direction (E_{ZZ}, vertical axis) based on the following regression model[19]:

$$E_{ZZ} = -81.9 + 3850\ \text{BMD},\ r^2 = 0.76,\ n = 76 \qquad (2)$$

where BMD is the bone mineral density. An upper limit for E_{ZZ} of 1 GPa was used for the trabecular bone.[21] The elastic–plastic material definitions for the trabecular bone elements were derived using 8 points along a normalized (stress divided by modulus) stress–strain curve measured empirically for 40 cylindri-

Table 1. Anisotropy Constants for Human Vertebral Trabecular Bone. The Young's Moduli E_{XX} and E_{YY} and Shear Moduli (G_{XY}, G_{XZ}, G_{YZ}) are Assigned as Fractions of the Longitudinal Modulus E_{ZZ}[32]

Ratio	Anisotropy Constant	Ratio	Anisotropy Constant
E_{ZZ}	1		
E_{XX}/E_{ZZ}	0.42	G_{XY}/E_{ZZ}	0.153
E_{YY}/E_{ZZ}	0.287	G_{XZ}/E_{ZZ}	0.131
ν_{XY}	0.226	G_{YZ}/E_{ZZ}	0.183
ν_{ZX}	0.399	ν_{ZY}	0.381

E_{ZZ} = on-axis modulus (vertical modulus).

cal core specimens.[20] The eight normalized stress values were then multiplied with the modulus of each element resulting in unique elastic–plastic material definitions for each element. The remaining orthotropic elastic constants for the trabecular bone were assigned based on literature data[32] for human vertebral trabecular bone (Table 1).

The cortical shell and endplates were modeled as an isotropic continuous wall enclosing the trabecular centrum using 20-noded brick elements and were assumed to have a nominal thickness of 0.35 mm.[29,33] The vertebral cortical bone modulus (E = 2.31 GPa) was then calibrated so that the computed stiffness of the whole vertebral body finite-element model matched that of the same experimentally tested whole vertebral body. Poisson's ratio of 0.3 was assumed for the shell, and it was confirmed that results were insensitive to this parameter. The vertebral cortical bone failure properties were modeled as elastic–perfectly plastic having a yield strain of 0.84%,[6] based qualitatively on cortical bone behavior.

Two loading cycles were simulated in the finite-element model with vertical compressive displacement boundary conditions applied through the layers of PMMA similar to the experiment. Structural stiffness for the vertebral model was numerically determined as the initial linear response of the nonlinear analysis. The predicted ultimate load was taken as the maximum load after which the load no longer increased on consecutive increments.

Elements of cortical or trabecular bone in the finite-element model that exceeded the compressive yield strain during the nonlinear analysis of the first loading cycle were considered to be damaged beyond yield. The elastic properties of the damaged trabecular bone elements were then reduced according to empirical relations developed for human vertebral trabecular bone (Figure 2) with a maximum percent reduction of 85%.[17] Trabecular bone elastic properties of elements strained below the yield point were reduced also using the above-mentioned criteria; however, those elements were considered to be damaged below yield. Young's moduli of cortical bone elements that exceeded the yield point during the first loading phase were reduced to the secant modulus (perfect damage modulus) measured at the maximum strain level reached. This correlation suggests that damage is a primary mechanism for the modulus reduction rather than plastic deformation, as experimentally investigated by Courtney et al.[11]

The reloading modulus of a single trabecular bone element along the vertical axis (E_{RELOAD}) depended on the total strain (ϵ_{TOT} in percent, as defined in Figure 2) to which the specimen was initially loaded along that axis. The elastic properties in the transverse plane were similarly scaled, maintaining the anisotropy ratios shown in Table 1. For cortical bone the reloading modulus was based on the perfect damage modulus (E_{PDZZ}; secant modulus drawn from point of unloading to origin) along the vertical axis for elements that had yielded[11]:

$$E_{RELOAD} = 1.35\ E_{PDZZ} - 7.68\ (r^2 = 0.81, n = 28) \quad (3)$$

After the elastic constants of the yielded elements had been replaced with the reduced properties, a second loading cycle was simulated and structural stiffness of the damaged vertebral body model was computed using a linear analysis. Stiffness reduction (%ΔS) was calculated in the same way as shown in Equation 1. The following analyses of different vertebroplasties were then performed using this damaged vertebral body model as a starting point.

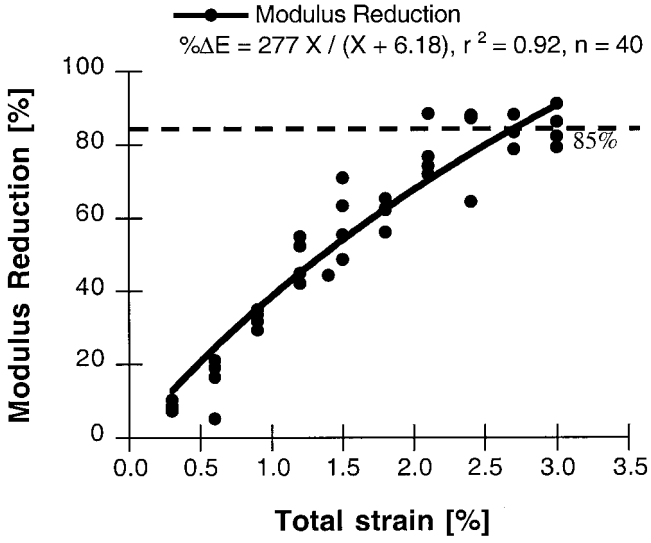

Figure 2. Percent modulus reduction after the initial loading cycle as a function of the total strain applied in the vertical axis. The data were extracted from measurements of cylindrical cores of human vertebral trabecular bone tested previously in compression.[17] The maximum percent reduction of the elastic modulus was limited to 85%.

Vertebroplasty Simulation. Four surgical vertebroplasty approaches were simulated by varying the distribution of PMMA introduced into the damaged vertebral body (Figure 3). The amount of PMMA (between 1 and 7 cm^3) virtually implanted into the damaged vertebral body was based on data obtained from *in vitro* experiments[2,31,36] and clinical trials of a balloon augmentation procedure (73 surgeries, internal database, Kyphon Inc., Santa Clara, CA). The shape of the injected PMMA was approximated with a cylinder having rounded edges.

For each of the four vertebroplasty simulations, four different volumes of PMMA (1, 3.5, 5, and 7 cm^3) were investigated resulting in a total of 16 different cases. For the bipedicular case the total PMMA volume simulated for the unipedicular case was repeated for the contralateral side. The corresponding percent fills of PMMA to whole vertebral body volume were 2%, 4%, 14%, 19%, and 28%, respectively. After virtual implantation of the bone cement in the damaged model, the resulting stiffness of the whole vertebra was computed for the various volumes of the implanted cement using linear finite-element analyses. Because *in vivo* boundary conditions at the endplate are a combination of displacement and stress boundary condi-

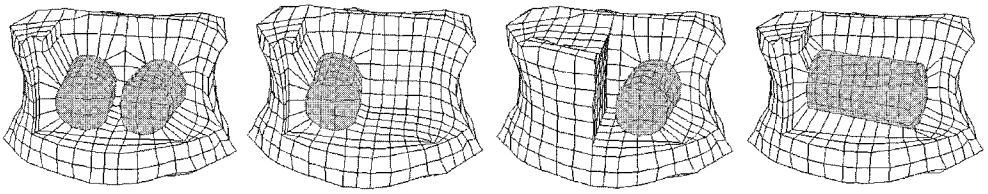

Figure 3. Finite-element mesh with two PMMA capsules (shaded) simulating bipedicular vertebroplasty. The trajectory of the PMMA was aligned with a pedicle angle of 22° for both sides. Simulating the unpedicular case, one PMMA capsule was inserted either on the right or the left side. A posterolateral angle of 70° was used for the posterolateral vertebroplasty with one capsule centered in the vertebral body. In the horizontal plane the PMMA was aligned parallel with the endplates. The model consisted of 1816 20-noded brick finite elements. For clarity, the endplates, cortical shell, and molded PMMA above the endplates are not shown.

tions imposed by the disc, we were concerned that the above simulations, where a rigid displacement was imposed, may not adequately capture the physiological behavior. To address this, we repeated all simulations of the vertebroplasty using a uniform compressive stress (pressure) boundary condition with a load equivalent to the reaction force measured experimentally at the yield point of the whole specimen. This allowed the endplate to toggle when loaded. Translation and rotation of the superior vertebral endplate relative to its unloaded state were calculated using conventions based on published experiments that used motion analysis techniques.[26]

■ Results

Comparison of the load–deformation curve between model and experiment revealed excellent qualitative agreement between the two. The predicted strength of the intact vertebral body of 2590 N was 14% lower than the experimentally measured value. Reduction of the elastic constants of the yielded elements produced a stiffness upon reloading of 7139 N/mm, a reduction of 24% compared with the initial stiffness. In the experiment a stiffness reduction of 33% for this specific vertebral body was measured. Considering the complexity of this nonlinear system, this level of agreement between model and experiment provided adequate validation of the simulation for the purpose of performing a comparative parameter study.

At the applied overall strain of 1.78%, almost one third of the volume of the vertebral body was predicted

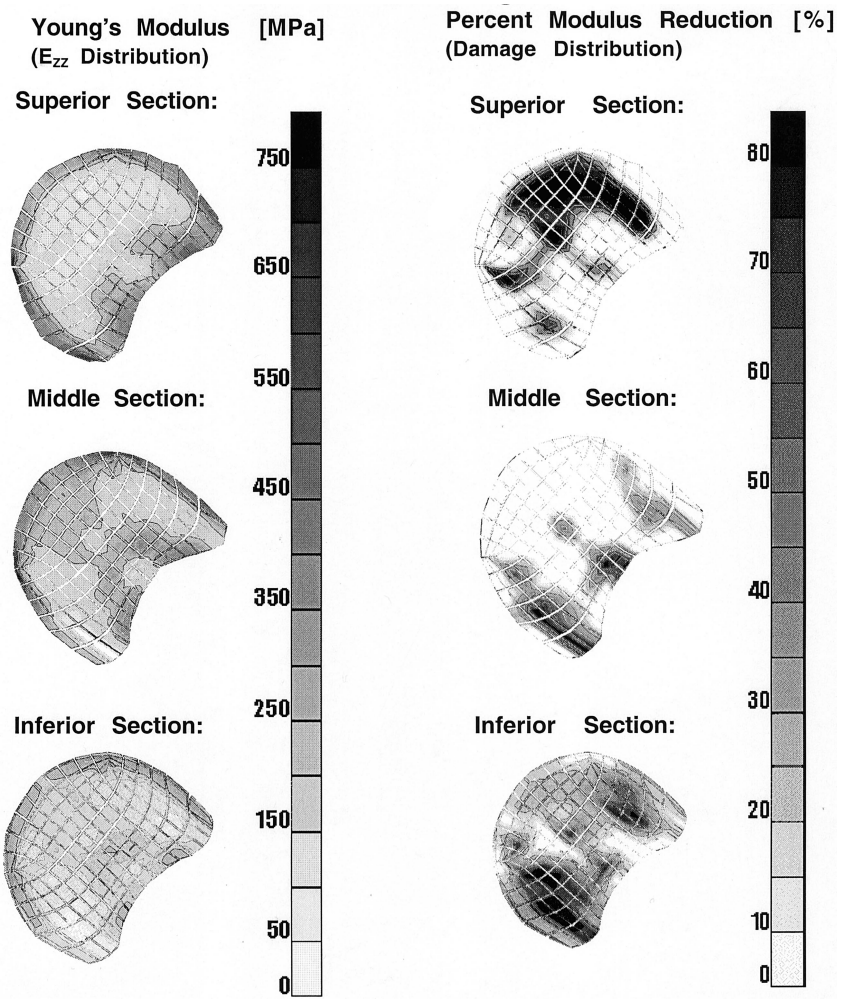

Figure 4. Spatial distribution of initial modulus and percentage modulus reduction (*i.e.*, extent of damage) for different transverse sections of the vertebral body. Top, Superior region of the vertebral body. Bottom, Inferior region. Note that the damage was predicted to occur on the left side more often in the posterior portion of the model, whereas on the right side the damage was present more anteriorly.

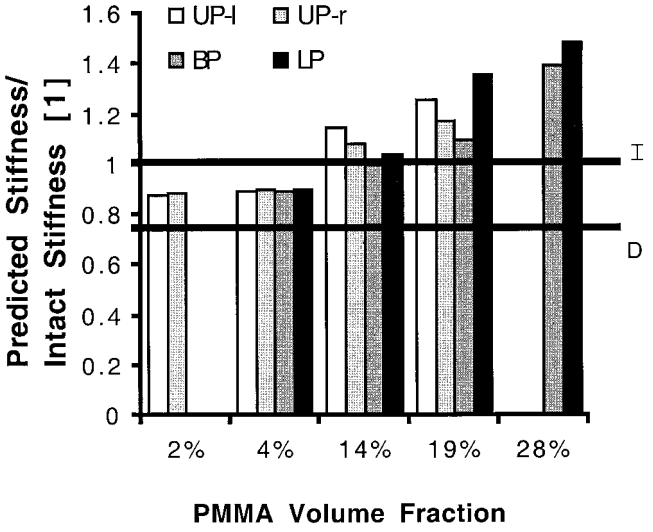

Figure 5. Normalized stiffnesses (divided by intact stiffness) *versus* volume of implanted bone cement compared with total vertebral volume. LP = lateral–posterior approach; BP = bipedicular approach; UP = unipedicular approach right; UP2 = unipedicular approach left; I and D = values without cement augmentation for the intact and damaged cases, respectively.

to contain damaged bone. The maximum strain detected was 18.5%. Slightly more elements yielded on the left (156) than on the right side (143) of the vertebral body (anteroposterior view), which was consistent with a difference in initial elastic modulus distribution, and thus load transfer, between the two sides (Figure 4). There was also a recognizable difference in damage patterns between the superior and inferior regions. In the superior region damage was close to the anterior cortical shell,

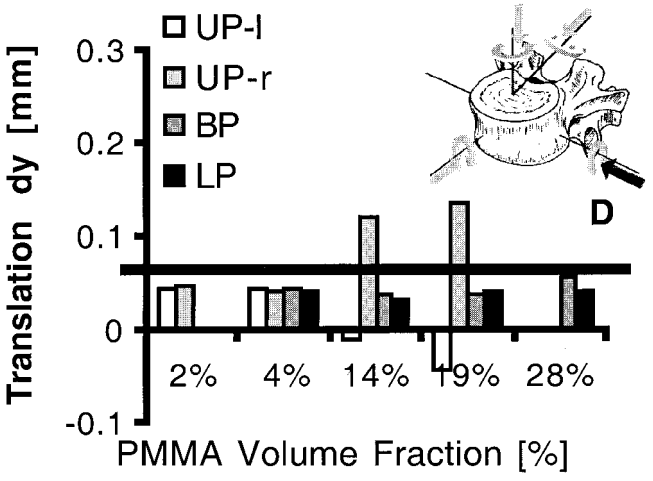

Figure 6. Displacement parameters were obtained from the vertebroplasty study of the superior endplate relative to the unloaded condition in the anterior direction, lateral direction to the right (viewing in the anterior–posterior direction), superior direction, and the overall translation with no specific orientation. Notable differences in translation were only found in the lateral direction between vertebroplasty procedures. Positive sign is indicated by direction of the dark arrow in the icon. D = values without cement augmentation for the damaged case.

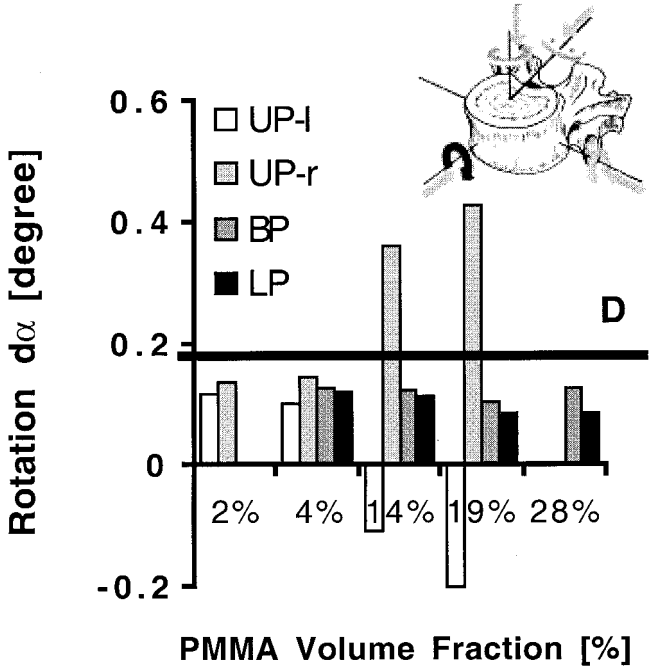

Figure 7. Angular displacement vectors were obtained from the vertebroplasty study relative to the unloaded condition in the horizontal plane, frontal plane, sagittal plane, and the overall rotational displacement with no specific orientation. Notable differences in rotational displacement were only found in the sagittal plane between vertebroplasty procedures. Positive sign is indicated by direction of the dark arrow in the icon. D = values without cement augmentation for the damaged case.

whereas in the inferior region damage was more concentrated to the posterolateral side (Figure 4).

Stiffness recovery after virtual vertebroplasty was strongly influenced by the volume fraction of the implanted cement, and less so by its distribution. The least amount of bone cement (2% fill) restored stiffness of the whole vertebral body to within 15% of the intact value (Figure 5). Fourteen percent fill (3.5 cm^3) restored the vertebral stiffness to its initial value, whereas 28% fill (7 cm^3) increased stiffness to almost 50% above the intact value. In terms of distribution, the posterolateral approach resulted in all four cases (4–28% fill) in a higher stiffness than the bipedicular approach. These differences were negligible for the low volume fraction cases but were higher as the volume of implanted bone cement increased. In all four cases the unipedicular simulations resulted in equal or higher stiffness predictions as the bipedicular or posterolateral cases. Predicted stiffness for the left and right vertebroplasty simulations were within 1.1% of each other for low PMMA volume fraction. For the highest PMMA volume fraction the unipedicular vertebroplasty on the right side was the stiffest case overall.

Asymmetric distribution of the cement, although providing good stiffness recovery, resulted in unstable conditions under pressure load due to the single-sided load transfer. When pressure boundary conditions were applied, the relative motion of the superior endplate to the unloaded state differed considerably for the unipedicular

cases when compared with the bipedicular or posterolateral cases for high volume fractions. An increase in bone cement fill from 4% to 14% caused an increase in rotation and translation in the frontal plane even beyond the values for the nontreated vertebral body (Figures 6 and 7). As expected, the least amount of rotation (toggle) and translation was observed for the bipedicular case for the high volume fraction of PMMA. Rotation and translation were always highest in the sagittal plane.

■ Discussion

We performed a comprehensive finite-element analysis to provide a theoretical framework for understanding and optimizing the biomechanics of the vertebroplasty procedure. We found that only a small amount of bone cement (~15% volume fraction of fill) is necessary to restore compressive stiffness of the damaged vertebral body to its value before damage. Furthermore, modest increases in volume of the cement can substantially increase vertebral stiffness beyond its intact value. These results agree closely with those from *in vitro* vertebroplasty experiments performed on 60 vertebral bodies by Belkoff et al[1] who found that only between 5 and 6 cm^3 of bone filler material (Orthocomp, Orthovita, Malvern, PA) in a bipedicular vertebroplasty approach is needed to restore stiffness and strength after a compression fracture in the thoracolumbar spine. We also found a tendency for increased toggle when cement was introduced through just one pedicle (unipedicular approach). Currently, there is no information available on how stiff or strong a treated vertebral body should be after vertebroplasty. Our results suggest that if the goal is to restore vertebral compressive stiffness to its predamage level, then only about 15% volume fill is required, and this may be best introduced via bipedicular or posterolateral approaches because they should minimize toggle due to their symmetric placement of the cement. Our results also suggest that with current clinical protocols, in which volume fractions of up to 30% are typically used, the resulting stiffness may be well beyond that of the intact vertebral body. Taken together, these results provide unique insight into how bone cement might best be used to repair a damaged vertebral body.

These results are plausible for a number of reasons. First, use of finite-element analysis enabled parameters such as cement volume and distribution to be controlled in a manner that would not be possible with experimental or animal models. Second, the model itself was highly anatomically detailed, with geometric and material properties derived from CT scans. Anisotropic elastic properties were used for the trabecular bone, and empirical relations from our previous work on the behavior of damaged trabecular bone[17] were used to model the modulus reductions associated with the damage from the initial overload. The resulting model was calibrated for elastic behavior against experimental data, and, considering the complexity of the overall system, predicted well the monotonic strength and reduction in stiffness upon reloading. The predicted damage locations within the bone were in the same regions as has been observed in *in vitro* experiments,[5,14] and the predicted asymmetric damage distribution along the superior–inferior axis has been noticed in experimental studies[5] in which superior endplate fractures occur more often than inferior fractures. And third, we addressed both changes in stiffness, which required use of displacement boundary conditions, and changes in displacement (*e.g.*, development of rotation or toggle), which required use of stress boundary conditions.

There are, however, a number of caveats. First, we addressed only the response to uniaxial compressive load. Thus, the damage produced in the model and the stiffness measured used as the output parameter were both in response to a purely compressive load. Given the complexity of the system and the dearth of information available on vertebroplasty biomechanics, the uniform compression case was considered adequate for the purposes of providing insight into the underlying mechanisms of this procedure. *In vivo* loading of the spine, however, is complex, including a substantial bending component.[27] Even so, it is not clear if the vertebral body experiences much bending with a healthy disc because in that case most of the load imparted to the endplates away from anulus is composed of a (uniform) pressure.[24,30] Our stress-based boundary conditions were included to address this situation. Thus, although we expect the same relative trends from this study to apply to more complex loading conditions, further work is required to quantify the magnitude of the effects and confirm the trends reported here. A second caveat is that our analysis was performed on a single vertebral body, that of an L1 vertebra from a 73-year-old female. This was a typical bone of the patient population at risk for spinal fracture.[15,18,34] Because factors such as age, sex, and disease can vary the geometric and material properties of vertebral bodies considerably, the issue arises as to the generality of the trends reported here. Experiments on the reductions in mechanical properties of whole vertebral bodies after an overload have demonstrated that the amount of damage does not depend on bone density but mostly on the magnitude of the applied strain.[21] Thus, we do not expect the trends reported here to vary much across different individuals for the same loading conditions. Regarding the magnitude of the applied strain used here (1.78%), it produced damage (modulus reductions) to some degree in about one third of the vertebral body volume, and the force–deformation curve had exceeded its ultimate point. The strain levels that cause fractures *in vivo* are not known; thus, it is difficult to put this applied strain in a functional context. Furthermore, it is not clear whether the regions of damage would extend at higher strain levels or whether just more severe damage would be imposed in the already damaged regions. This remains an important topic for further research because the biomechanics of the vertebroplasty are directly related to the damage morphology.

Contrary to the only available biomechanics literature on this topic,[31] our results suggest that unipedicular vertebroplasty may not be as effective in recovering vertebral body stability as bipedicular or posterolateral vertebroplasty. The differences in effectiveness of unipedicular vertebroplasty predicted by the computer model used in this study and the experimental study performed by Tohmeh et al[31] can be explained by differences in boundary conditions. Tohmeh et al[31] performed a uniaxial compression test on vertebral bodies treated with unipedicular or bipedicular vertebroplasty and concluded that both approaches are biomechanically equivalent. Our analysis agreed with this finding, but only when displacement boundary conditions were used. By contrast, when pressure (uniaxial compressive stress) boundary conditions were applied, the compliance of the unsupported side became evident as this side preferentially deformed, resulting in medial–lateral toggling in the frontal plane. Thus, use of both displacement and pressure boundary conditions appears to be necessary to characterize both stiffness and stability of vertebroplasty constructs.

Clinically, the optimal configuration for vertebroplasty is not yet clear, although the results of this analysis provide unique insight into possible improvements. Our data suggest that only a relatively small amount of bone cement is needed to restore stiffness to predamage levels and that greater filling can result in substantial increases in stiffness (beyond intact levels). The question then arises as to how much bone cement filler should be used. Based on the experience with posterior stabilization systems,[12,22] one possible concern with overfilling is that an overly stiff vertebral body may compromise the kinematics of the surrounding motion segments. With vertebroplasty, because only the vertebral body is stiffened and the disc undergoes most of the deformation during activities such as forward flexion,[4,37] and given that the vertebra is much stiffer than the disc, it is unlikely that an increase in vertebral stiffness will have an appreciable effect on the kinematics of adjacent motion segments. Thus, biomechanically, use of a large volume of cement is unlikely to present problems to the adjacent vertebrae, although it may increase risk of leakage depending on how the procedure is performed surgically. Our data also suggest that use of a large filling fraction renders the system more sensitive to the placement of the cement because asymmetric distributions with large filling volumes can promote single-sided load transfer and thus toggle. Taken together, these results suggest that large volume fractions may not be the most biomechanically optimal configuration, and an improvement might be achieved by use of lower fills with symmetric placement. In theory, this strategy should restore stiffness to predamage levels while minimizing risk of complications due to surgical factors such as leakage.

Acknowledgment

The authors thank David Kopperdahl, PhD, for providing the experimental data.

■ Key Points

- Vertebroplasty is an effective tool in recovery of vertebral stiffness and strength after fracture.
- Only a small amount of bone cement is needed in vertebroplasty to recover vertebral stiffness to its initial/intact value.
- Symmetric placement of bone filler material in vertebroplasty is recommended.
- Experimental studies on vertebroplasty should include bending compliance analysis.

References

1. Belkoff S, Deramond H, Mathis J, Jasper L. Vertebroplasty: the biomechanical effect of cement volume. Trans Orthop Res Soc 2000;46:356.
2. Belkoff SM, Mathis JM, Erbe EM, Fenton DC. Biomechanical evaluation of a new bone cement for use in vertebroplasty. Spine 2000;25:1061–4.
3. Brado M, Hansmann HJ, Richter GM, Kauffmann GW. Interventional therapy of primary and secondary tumors of the spine. Orthopaede 1998;27:269–73.
4. Brault JS, Driscoll DM, Laakso LL, et al. Quantification of lumbar intradiscal deformation during flexion and extension, by mathematical analysis of magnetic resonance imaging pixel intensity profiles. Spine 1997;22:2066–72.
5. Brinckmann P, Biggeman M, Hilweg D. Fatigue fracture of human lumbar vertebrae. Clin Biomech 1988;3(suppl):1–23.
6. Carter DR, Caler WE, Spengler DM, Frankel VH. Fatigue behavior of adult cortical bone: the influence of mean strain and strain range. Acta Orthop Scand 1981;52:481–90.
7. Chiras J, Depriester C, Weill A, et al. Percutaneous vertebral surgery: technics and indications. J Neuroradiol 1997;24:45–59.
8. Cortet B, Cotton A, Boutry N, et al. Percutaneous vertebroplasty in patients with osteolytic metastases or multiple myeloma. Rev Rhum Engl Ed 1997;64:177–84.
9. Cotton A, Boutry N, Cortet B, et al. Percutaneous vertebroplasty: state of the art. Radiographics 1998;18:311–20.
10. Cotton A, Dewatre F, Cortet B, et al. Percutaneous vertebroplasty for osteolytic metastases and myeloma: effects of the percentage of lesion filling and the leakage of methyl methacrylate at clinical follow-up. Radiology 1996;200:525–30.
11. Courtney AC, Hayes WC, Gibson LJ. Age-related differences in post-yield damage in human cortical bone: experiment and model. J Biomech 1996;29:1463–71.
12. Ferguson TL, Tencer AF, Woodard P, Allen BLJ. Biomechanical comparison of spinal fracture models and the stabilizing effects of posterior instrumentations. Spine 1988;13:453–60.
13. Gangi A, Kastler BA, Dietemann JL. CT-guided interventional procedures for pain management in the lumbosacral spine. Radiographics 1998;18:621–33.
14. Hansson T, Keller T, Jonson R. Fatigue fracture morphology in human lumbar motion segments. J Spinal Disord 1988;1:33–8.
15. Hayes WC, Piazza SJ, Zysset PK. Biomechanics of fracture risk prediction of the hip and spine by quantitative computed tomography. Radiol Clin North Am 1991;29:1–18.
16. Jensen ME, Evans AJ, Mathis JM, et al. Percutaneous polymethylmethacrylate vertebroplasty in the treatment of osteoporotic vertebral body compression fractures: technical aspects. Am J Neuroradiol 1997;18:1897–904.
17. Keaveny TM, Wachtel EF, Kopperdahl DL. Mechanical behavior of human trabecular bone after overloading. J Orthop Res 1999;17:346–53.
18. Keller TS. Increased risk of fracture associated with changes in vertebral structure in the aging spine. Proc Bioeng Conf ASME BED 1995;29:305–6.
19. Kopperdahl DL. Structural consequences of damage on the mechanical behavior of the human vertebral body. Ph.D. dissertation, University of California, Berkeley, 1998.

20. Kopperdahl DL, Keaveny TM. Yield strain behavior of trabecular bone. J Biomech 1998;31:601–8.
21. Kopperdahl DL, Pearlman JL, Keaveny TM. Biomechanical consequences of an isolated overload on the human vertebral body. J Orthop Res 2000;18: 685–90.
22. Kornblatt MD, Casey MP, Jacobs RR. Internal fixation in lumbosacral spine fusion: a biomechanical and clinical study. Clin Orthop 1986;203:141–50.
23. Martin JB, Jean B, Sugiu K, et al. Vertebroplasty: clinical experience and follow-up results. Bone 1999;25(suppl):11–5.
24. McNally DS, Arridge RG. An analytical model of intervertebral disc mechanics. J Biomech 1995;28:53–68.
25. Padovani B, Kasriel O, Brunner P, Peretti-Viton P. Pulmonary embolism caused by acrylic cement: a rare complication of percutaneous vertebroplasty. Am J Neuroradiol 1999;20:375–7.
26. Panjabi MM, Krag MH, Goel VK. A technique for measurement and description of three-dimensional six degree-of-freedom motion of a body joint with an application to the human spine. J Biomech 1981;14:447–60.
27. Panjabi MM, Pelker RR, White AA. Biomechanics of the spine. In: Wilkins RH, Rengachary SS, eds. Neurosurgery, 2nd ed., vol. 3. New York: McGraw-Hill, 1996:3751–60.
28. Perrin C, Jullien V, Padovani B, Blaive B. Percutaneous vertebroplasty complicated by pulmonary embolus of acrylic cement. Rev Mal Respir 1999;16: 215–7.
29. Silva MJ, Keaveny TM, Hayes WC. Direct and computed tomography thickness measurements of the human lumbar vertebral shell and endplate. Bone 1994;15:409–14.
30. Tadano S, Katagiri K, Umehara S, Ukai T. A constitutive modeling of the human lumbar intervertebral disc and forward-backward bending simulation. Biomed Mater Eng 1997;7:179–91.
31. Tohmeh AG, Mathis JM, Fenton DC, Levine AM, Belkoff SM. Biomechanical efficacy of unipedicular versus bipedicular vertebroplasty for the management of osteoporotic compression fractures. Spine 1999;24:1772–6.
32. Ulrich D, Van Rietbergen B, Laib A, Rueegsegger P. The ability of three-dimensional structural indices to reflect mechanical aspects of trabecular bone. Bone 1999;25:55–60.
33. Vesterby A, Mosekilde L, Gundersen HJG, et al. Biologically meaningful determinants of the in vitro strength of lumbar vertebrae. Bone 1991;12: 219–24.
34. von der Recke P, Hansen MA, Overgaard K, Christiansen C. The impact of degenerative conditions in the spine on bone mineral density and fracture risk prediction. Osteoporos Int 1996;6:43–9.
35. Weill A, Chiras J, Simon JM, et al. Spinal metastases: indications for and results of percutaneous injection of acrylic surgical cement. Radiology 1996; 199:241–7.
36. Wilson DR, Myers ER, Mathis JM, et al. Effect of augmentation on the mechanics of vertebral wedge fractures. Spine 2000;25:158–65.
37. Yoganandan N, Cusick JF, Pintar FA, Droese K, Reinartz J. Cyclic compression-flexion loading of the human lumbar spine. Spine 1994;19:784–90; discussion 91.

Address reprint requests to

Tony M. Keaveny, PhD
6175 Etcheverry Hall
University of California
Berkeley, CA 94720-1740
E-mail: tmk@me.berkeley.edu

View publication stats